which should be cited to refer to this work.

Hydrogen storage properties of Mg[BH$_4$]$_2$

T. Matsunaga [a,b,*], F. Buchter [a,b], P. Mauron [a,b], M. Bielman [a,b], Y. Nakamori [c],
S. Orimo [c], N. Ohba [d], K. Miwa [d], S. Towata [d], A. Züttel [a,b]

[a] *EMPA, Department Environment, Energy and Mobility, Abt. 138 "Hydrogen & Energy", Überlandstrasse 129, 8600 Dübendorf, Switzerland*
[b] *University of Fribourg, Physics Department, Pérolles, 1700 Fribourg, Switzerland*
[c] *Institute for Materials Research, Tohoku University, Sendai 980-8577, Japan*
[d] *Toyota Central Research and Development Laboratories, Inc., Nagakute, Aichi 480-1192, Japan*

Abstract

Among the large variety of possible complex hydrides only few exhibit a large gravimetric hydrogen density and stability around $40\,\mathrm{kJ\,mol^{-1}H_2}$. Mg[BH$_4$]$_2$ is based on theoretical approaches a complex hydride with an equilibrium hydrogen pressure of approximately 1 bar at room temperature and a hydrogen content of 14.9 mass%. The reaction of Li[BH$_4$] with MgCl$_2$ at elevated temperatures was investigated as a possible route to synthesize Mg[BH$_4$]$_2$. Li[BH$_4$] reacts with MgCl$_2$ at a temperature >523 K at a pressure of 10 MPa of hydrogen, where the product contains LiCl and Mg[BH$_4$]$_2$. The desorption pc-isotherm of the product obtained at 623 K shows two flat plateaus, which indicates that the decomposition of the product consists of a two-step reaction. The products of the first and the second decomposition reaction were analyzed by means of X-ray diffraction and found to be MgH$_2$ and Mg, respectively. The enthalpy for the first decomposition reaction was determined to be $\Delta H = -39.3\,\mathrm{kJ\,mol^{-1}H_2}$ by the Van't Hoff plot of the equilibrium measurements between 563 K and 623 K, which is significantly lower than that for pure Li[BH$_4$] ($\Delta H = -74.9\,\mathrm{kJ\,mol^{-1}H_2}$). However, only the second reaction step (MgH$_2 \rightarrow$ Mg) is reversible at the condition up to 623 K at 10 MPa of hydrogen.

Keywords: Hydrogen absorbing materials; Thermodynamic properties; Thermal analysis

1. Introduction

Hydrogen storage technology is one of the most important subjects for the introduction of fuel cell vehicles in transportation. The hydrogen storage density as well as the moderate operating temperatures for desorption and absorption of hydrogen are key parameters for an onboard storage system. Complex hydrides, consisting of light elements, are very promising materials for hydrogen storage because of their high gravimetric and volumetric hydrogen density [1]. Since Bogdanovic and Schwickardi reported the reversibility of the catalyzed hydrogen sorption reaction of NaAlH$_4$ [2], many efforts have been made to investigate complex hydrides as hydrogen storage materials [3–7]. Besides the basic physical properties, the challenges are to tailor the stability and to improve the reversibility of the hydrogen sorption reaction of complex hydrides.

The hydrogen in the complex hydrides is located in the corners of a tetrahedron with B or Al in the center. The negative charge of the anion, [BH$_4$]$^-$ and [AlH$_4$]$^-$, is compensated by a cation, e.g., Li or Na. The bonding character and the physical properties of the complex hydrides are largely determined by the difference in electronegativity between the cation and boron or aluminum, respectively. From this point of view, first-principles calculations [8,9] and experimental studies [10] on the stability of complex hydrides have been performed. Recently, Nakamori et al. have investigated the relation between stability of borohydrides and electronegativity of cations for various borohydrides and have shown that there is a good correlation between them [11].

Magnesium borohydride (Mg[BH$_4$]$_2$) is a very promising material for hydrogen storage because of its high gravimetric storage density (14.9 mass%). The Pauling electronegativity of magnesium is 1.31, which is greater than that of lithium (0.98), therefore, it is expected that Mg[BH$_4$]$_2$ is less stable than

* Corresponding author at: EMPA, Department Environment, Energy and Mobility, Abt. 138 "Hydrogen & Energy", Überlandstrasse 129, 8600 Dübendorf, Switzerland. Tel.: +41 44 823 4038; fax: +41 44 823 4022.
E-mail address: tomoya@matsunaga.tec.toyota.co.jp (T. Matsunaga).

Li[BH$_4$]. However, properties of Mg[BH$_4$]$_2$ as a hydrogen storage material, especially thermodynamic property, are not known yet and the investigation requires sophisticated instruments and a well-defined sample. Stasinevich and Egorenko investigated the stability of various borohydrides by means of thermal analysis in hydrogen pressures up to 1.0 MPa [12]. They reported that hydrogen desorption from Mg[BH$_4$]$_2$ occurs at 586–596 and 683–693 K, where the former corresponds to the desorption from Mg[BH$_4$]$_2$ to MgH$_2$, the latter from MgH$_2$ to Mg. Konoplev and Bakulina also investigated the thermal analysis of Mg[BH$_4$]$_2$, where they mentioned that Magnesium boride (MgB$_2$) may be formed after thermal decomposition [13]. Direct synthesis of Mg[BH$_4$]$_2$ from Magnesium, boron and hydrogen has been reported by Goerrig [14], where it has been claimed that Mg[BH$_4$]$_2$ can be formed from these elements at 923 K and 15 MPa of hydrogen.

In this study, the reaction of Li[BH$_4$] with MgCl$_2$ at elevated temperatures is investigated as a new route to synthesize Mg[BH$_4$]$_2$. Lithium borohydride and magnesium chloride are used as starting materials. The reactions of Li[BH$_4$] with MgCl$_2$ are examined by differential scanning calorimetry (DSC). The synthesis products as well as the hydrogen desorption products are investigated by X-ray diffraction and Raman spectroscopy. Hydrogen desorption and absorption property of the synthesis product is investigated by temperature programmed desorption (TPD) and pc-isotherm measurement. Based on the equilibrium pressures of measured pc-isotherms the dehydrogenation enthalpy and entropy were computed by means of the Van't Hoff equation.

2. Experimental

The starting materials used in this study were purchased from Aldrich Co. Ltd.: The purities are >95% for Li[BH$_4$] and >99.9% for MgCl$_2$, respectively. The samples were handled in pure argon atmosphere (glove box), in high vacuum and under pure hydrogen gas in order to avoid any possible contamination by moisture or oxygen from air.

2.1. Reaction of Li[BH$_4$] with MgCl$_2$

The reaction of Li[BH$_4$] with MgCl$_2$ was investigated by differential scanning calorimetry (DSC) (Mettler Toledo Inc. HP DSC827e). Five milligrams of the sample (for 2:1 mole ratio) was mixed in an argon glove box and filled in a DSC sample cell made of aluminum. The sample cell was sealed up in argon atmosphere. Therefore, it has never been exposed to any gases except pure argon during the measurement. The DSC measurement of Li[BH$_4$] and MgCl$_2$ mixture was carried out in the temperature range from 313 to 513 K at the heating (or cooling) rate of 5 K min^{-1} in the sealed sample cell for three heating and cooling cycles. Measurements with pure Li[BH$_4$] and MgCl$_2$ were also performed at the same heating condition.

Heat treatments of Li[BH$_4$] and MgCl$_2$ mixture were carried out in a stainless steel cylinder under 10 MPa of hydrogen at 453, 523 or 593 K. In each heat treatment, approximately 600 mg of Li[BH$_4$] and MgCl$_2$ mixture (for 2:1 mole ratio) was pressed in order to make a pellet and filled into a cylinder in an argon glove box. After evacuating by rotary vacuum pump for 1 h at room temperature, 10 MPa of hydrogen was introduced into the cylinder and heated up. It was kept at the final temperature mentioned above for 3 h and then slowly cooled to room temperature. Crystal structures of the samples after heat treatment were investigated at room temperature by powder X-ray diffraction measurement (SIEMENS, D-500, Cu Kα radiation). Raman spectra of the samples were measured at room temperature using a Dilor Labram Raman spectrometer equipped with a HeNe laser (632.8 nm) and an optical microscope. To avoid exposure to

air, each sample was filled into a sample holder in the argon glove box and covered with plastic wrap film during X-ray diffraction measurement and Raman spectroscopy measurement.

2.2. Hydrogen desorption and absorption

Hydrogen desorption property of the product synthesized by the heat treatment of Li[BH$_4$] with MgCl$_2$ (for 2:1 mole ratio) at 593 K under 10 MPa of hydrogen was investigated as follows.

Temperature programmed desorption (TPD) measurements were carried out in vacuum after the heat treatment in a stainless steel cylinder with a heating rate of 0.2–5.0 K min^{-1}. After the heat treatment, the samples were cooled down to room temperature under 10 MPa of hydrogen. Subsequently, hydrogen gas was extracted from the cylinder to vacuum at room temperature. The samples were heated up under vacuum from room temperature to 773 K. During the measurements, desorbed gas volume was measured using a mass flow controller (Brooks instruments, 5850E).

Desorption isotherms were measured at 563, 593 and 623 K using the same mass flow controller mentioned above. A total of 1.6 g of the sample were used for each measurement. Hydrogen pressure was decreased from 10 MPa to vacuum with a flow rate of 1.0 cm^3 min^{-1}. It took approximately 70 h to perform each desorption measurement with this gas flow rate. Absorption isotherm measurement was performed at 623 K continuously after the desorption measurement at the same temperature. Hydrogen was filled into the cylinder with a flow rate of 1.0 cm^3 min^{-1} until the pressure was increased up to 10 MPa.

After desorption or absorption measurement, the cylinder was cooled down to room temperature. The samples were taken out in an argon glove box. Crystal structures of the samples were investigated by powder X-ray diffraction measurement as mentioned above at room temperature.

3. Results and discussion

3.1. Reaction of Li[BH$_4$] with MgCl$_2$

The DSC profiles of Li[BH$_4$] and MgCl$_2$ mixture are shown in Fig. 1. Profiles of pure Li[BH$_4$] and pure MgCl$_2$ were also investigated as references. For Li[BH$_4$], there is an endothermic peak (at $T = 386$ K, $\Delta Q = -206.0$ J g^{-1}) during heating from 313 to 513 K and an exothermic peak during cooling both of them corresponding to the phase transition of Li[BH$_4$], whereas no peak was observed for MgCl$_2$ in this temperature range. For the Li[BH$_4$] and MgCl$_2$ mixture sample, there is an endothermic peak (at $T = 385$ K, $\Delta Q = -56.3$ J g^{-1}) during the 1st heating procedure, corresponding to the phase transition of Li[BH$_4$]. However, this peak disappears after the cooling period of 1st cycle. This result is an evidence that there is no pure Li[BH$_4$] remains after the 1st heating. In addition, for the Li[BH$_4$] and MgCl$_2$ mixture, other exothermic and endothermic peaks are observed after the 1st cooling at $T = 440$ K ($\Delta Q = 23.6$ J g^{-1}). These peaks are not observed for pure Li[BH$_4$] or pure MgCl$_2$. This result implies that some reaction took place during the 1st heating. The endothermic peak at 440 K observed after the 1st cooling is in agreement with the DSC measurement result reported for Mg[BH$_4$]$_2$ [12]. Therefore, the following reaction during the 1st heating procedure is assumed:

$$2Li[BH_4] + MgCl_2 \rightarrow Mg[BH_4]_2 + 2LiCl$$
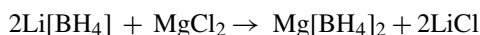
XRD measurement results after heat treatment also indicate that Li[BH$_4$] react with MgCl$_2$ during heat treatment. Fig. 2 shows the XRD measurement results after heat treatment at
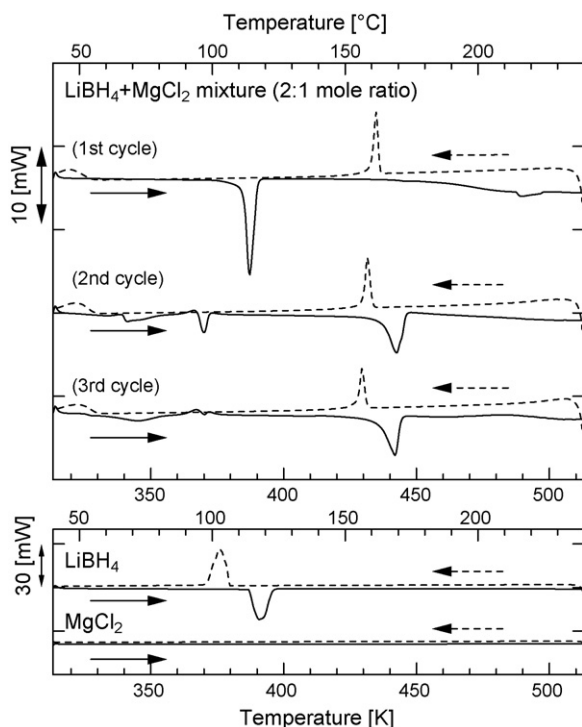
2

Fig. 1. Differential scanning calorimetry profiles of Li[BH$_4$] and MgCl$_2$ mixture with a sealed sample cell. The heating rate is 5 K min^{-1}. Measurements with pure Li[BH$_4$] and MgCl$_2$ were also performed at the same heating condition. Solid lines and dotted lines show heating and cooling, respectively. A total of 5 mg of the sample was used for each measurement.

various temperatures. Mixing Li[BH$_4$] and MgCl$_2$ in a mortar in an inert atmosphere (Ar) at room temperature does not lead to any reaction. However, after heat treatment, the peaks corresponding to Li[BH$_4$] and MgCl$_2$ disappear. New peaks were observed which correspond to LiCl. Although there is still a small amount of Li[BH$_4$] and MgCl$_2$ after heat treatment at 453 K, neither Li[BH$_4$] nor MgCl$_2$ was observed after
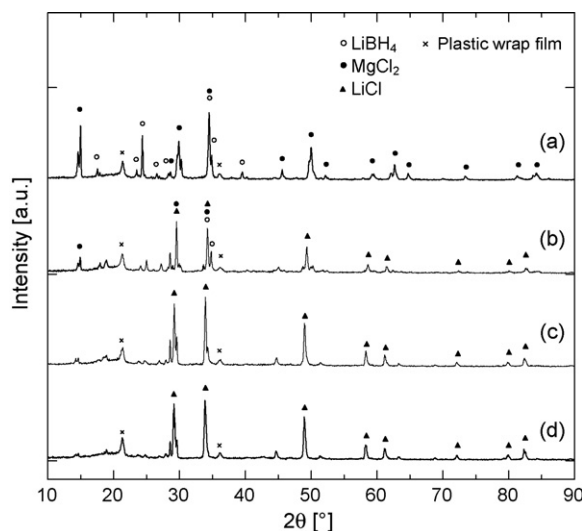
Fig. 2. Powder X-ray diffraction profiles of Li[BH$_4$] and MgCl$_2$ mixture: (a) before heat treatment; (b) after heat treatment at 453 K; (c) after heat treatment at 523 K; (d) after heat treatment at 593 K, respectively. Each heat treatment was carried out under 10 MPa of hydrogen.

heat treatment at the temperature >523 K. The X-ray diffraction peaks around $2\Theta = 18$–$19°$ after heat treatment at 453 K may be due to an intermediate compound of the reaction, which are not observed after heat treatment at higher temperatures.

The Raman spectra of pure Li[BH$_4$] are shown in Fig. 3(a and b) and Li[BH$_4$] with MgCl$_2$ after heat treatment at 593 K under 10 MPa of hydrogen in Fig. 3(c and d). The Raman shifts observed for pure Li[BH$_4$] (Fig. 3(a and b)) are in agreement with the bending mode and the stretching mode reported for [BH$_4$]$^{-}$ in Li[BH$_4$], respectively [15]. After heat treatment, two of new Raman shifts occurred at 1200 and 1380 cm^{-1} in the bending mode region as is shown in Fig. 3(c). The Raman spectra after heat treatment is consistent with the Raman spectra [11] and the IR spectra [13] reported for Mg[BH$_4$]$_2$. This result shows that Mg[BH$_4$]$_2$ is included in the product after heat treatment. In the stretching mode region, the splitting at 2300 cm^{-1} has disappeared after heat treatment as is shown in Fig. 3(d). Probably this spectrum shows overlap of stretching mode in Mg[BH$_4$]$_2$ and Li[BH$_4$] [11,15]. The product after the heat treatment at 593 K was also examined by DSC measurement. The result shows that there is an endothermic peak around 440 K, whereas no peak from LiBH$_4$ was observed. This result indicates that most of the product is supposed to be Mg[BH$_4$]$_2$.

3.2. Hydrogen desorption and absorption

3.2.1. Temperature programmed desorption

Fig. 4 shows the temperature programmed desorption spectra at a heating rate of 0.2 K min^{-1}. Although the product after heat treatment contains LiCl, LiCl does not decompose below 773 K. Therefore, all of the desorbed gas is supposed to originate from Mg(BH$_4$)$_2$. In addition, more than 99.7% of the desorbed gas from the sample was confirmed to be hydrogen by mass spectroscopy. The hydrogen desorption temperature of Li[BH$_4$] and MgCl$_2$ mixture after the heat treatment is approximately 100 K lower as compared to that of pure Li[BH$_4$]. The sample after heat treatment has two desorption peaks. It starts to decompose at 500 K and the first desorption peak appears around 563 K. This peak is dominant and more than half of hydrogen is evolved. The second desorption peak starts at 600 K and it is very sharp as compared to the first desorption peak. The shape of two independent desorption peaks implies that decomposition reaction consists of two steps.

Desorption spectra of Li[BH$_4$] and MgCl$_2$ mixture after heat treatment with different heating rates are shown in Fig. 5(a). The peak temperatures of the spectra were used to determine the activation energy of the first and the second desorption. The logarithm of the ratio of the heating rate divided by the square of the peak temperature is a linear function of the inverse temperature if the hydrogen desorption is a first order reaction (Fig. 5(b)). The slope of the fitted line corresponds to the activation energy for the reaction (Kissinger plot) [16]. The activation energy of the first and the second desorption obtained by Fig. 5(b) were 122 and 166 kJ mol^{-1}, respectively.
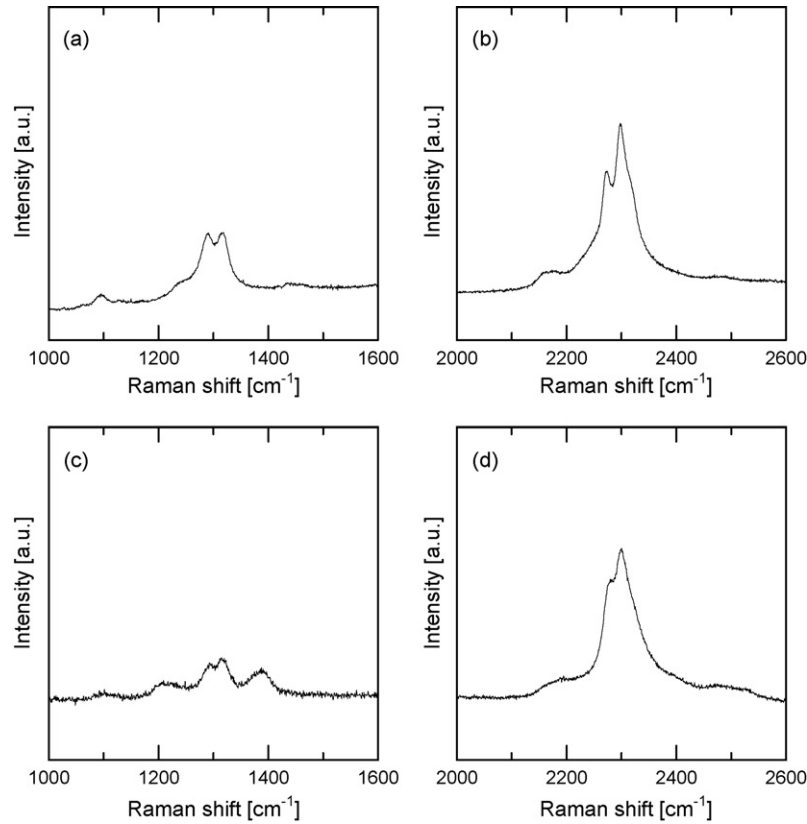
Fig. 3. Raman spectra of pure Li[BH$_4$] (a and b) and Li[BH$_4$] with MgCl$_2$ after heat treatment at 593 K under 10 MPa of hydrogen (c and d).
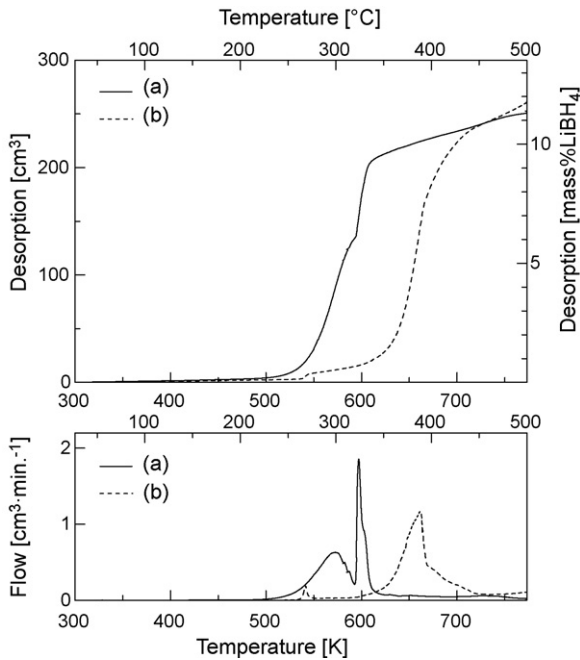

Fig. 4. Temperature programmed desorption spectra of: (a) Li[BH$_4$] and MgCl$_2$ mixture after heat treatment at 593 K under 10 MPa of hydrogen; (b) pure Li[BH$_4$]. The samples were heated after evacuation at room temperature with a heating rate of 0.2 K min^{-1}. The upper graph and the lower graph show the desorbed gas volume and the gas flow as a function of temperature, respectively.

3.2.2. PC desorption and absorption isotherms

Fig. 6 shows the pressure composition desorption isotherms at 563, 593 and 623 K. Two plateaus were observed at 623 K at more than 0.1 MPa, whereas only one plateau was observed at 563 and 593 K within this pressure range. Equilibrium pressures of the first desorption varied from 1.4 MPa at 563 K to 3.1 MPa at 623 K. The equilibrium pressure (P_{eq}) as a function of temperature is related to the changes ΔH and ΔS of enthalpy and entropy, respectively, by the Van't Hoff equation:

$$\ln\left(\frac{P_{eq}}{P_{eq}^0}\right) = \frac{\Delta H}{R}\frac{1}{T} - \frac{\Delta S}{R} \tag{1}$$

Based on the Van't Hoff plot shown in Fig. 7, the dehydrogenation enthalpy and entropy were found to be $\Delta H = -39.3$ kJ mol^{-1}H$_2$, $\Delta S = -91.3$ J mol^{-1} K^{-1}, respectively. Whereas the dehydrogenation enthalpy of pure Li[BH$_4$] is obtained to be $\Delta H = -74.9$ kJ mol^{-1}H$_2$ from the equilibrium pressure of Li[BH$_4$] reported in the literature [17]. Therefore, the product of Li[BH$_4$] with MgCl$_2$ after heat treatment is thermodynamically less stable than pure Li[BH$_4$].

Absorption pc-isotherm was measured at 623 K subsequently after the desorption measurement at the same temperature. As is shown in Fig. 6, only one absorption plateau was observed around 1.3 MPa, where the absorbed hydrogen amount was almost the same as the desorbed hydrogen amount in the second reaction step of the desorption measurement. This result
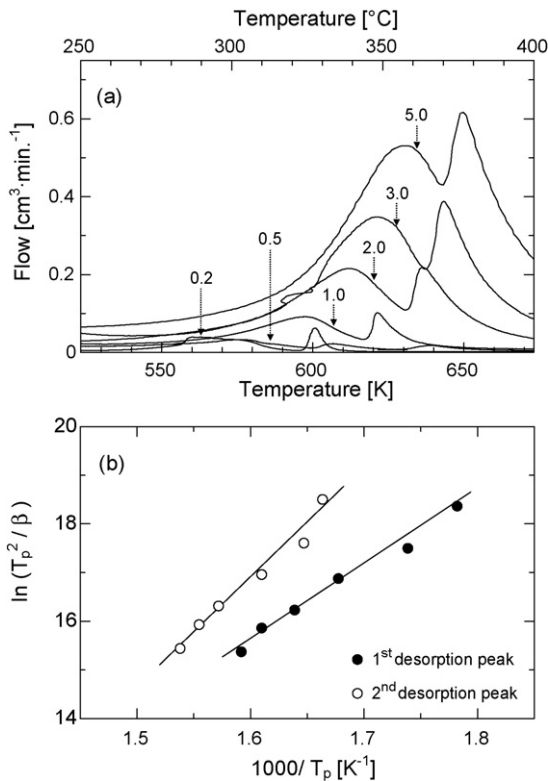
4

Fig. 5. (a) Temperature programmed desorption spectra of Li[BH$_4$] and MgCl$_2$ mixture after heat treatment at 593 K under 10 MPa of hydrogen. Numbers shown in the graph indicate the heating rate in K min^{-1}. A total of 20 mg of the sample was used for the measurements. (b) Kissinger plot of thermal desorption spectra at a heating rate of 0.2–5.0 K min^{-1}, where T_p is a peak temperature of the spectra and β is a heating rate.

is a clear evidence that only the second step of the reaction is reversible under this measuring condition.

3.2.3. X-ray diffraction analysis

Fig. 8 shows the XRD measurement results of the Li[BH$_4$] and MgCl$_2$ mixture (a) after heat treatment at 593 K for 3 h, (b)
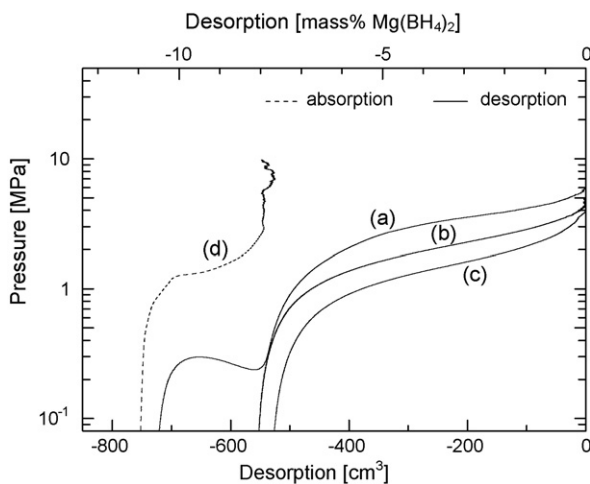

Fig. 6. Absorption/desorption isotherms for Li[BH$_4$] and MgCl$_2$ mixture after heat treatment at 593 K: (a) desorption at 563 K; (b) desorption at 593 K; (c) desorption at 623 K; (d) absorption at 623 K. Curve (d) was measured after the desorption measurement at the same temperature.
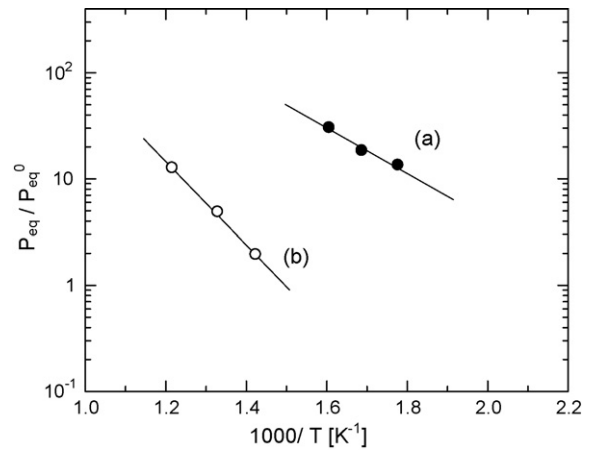

Fig. 7. Van't Hoff plots for (a) Li[BH$_4$] with MgCl$_2$ after heat treatment at 593 K and (b) pure Li[BH$_4$]. Equilibrium pressures of (a) and (b) are obtained from PC desorption isotherms in Fig. 5, from ref. [17], respectively.

after desorption in vacuum to 593 K, (c) after desorption in vacuum to 623 K and (d) after absorption up to 10 MPa of hydrogen at 623 K, respectively. As it is shown in Fig. 8(b), after desorption in vacuum to 593 K, the peaks which correspond to MgH$_2$ are observed, whereas the diffraction pattern of metallic Mg is not observed. On the other hand, as is shown in Fig. 8(c), after desorption in vacuum to 623 K, the peaks corresponding to Mg are clearly present, where the peaks from MgH$_2$ are no longer observed. These results indicate that MgH$_2$ desorbs hydrogen to be Mg during the second desorption step. After absorption up to 10 MPa of hydrogen at 623 K, as is shown in Fig. 8(d), MgH$_2$ forms again, which implies the hydrogenation of Mg during the absorption procedure. LiCl remains during desorption/absorption procedure as is shown in Fig. 8. Consequently, the overall results of X-ray diffraction analysis can be explained by the following two-step reaction:
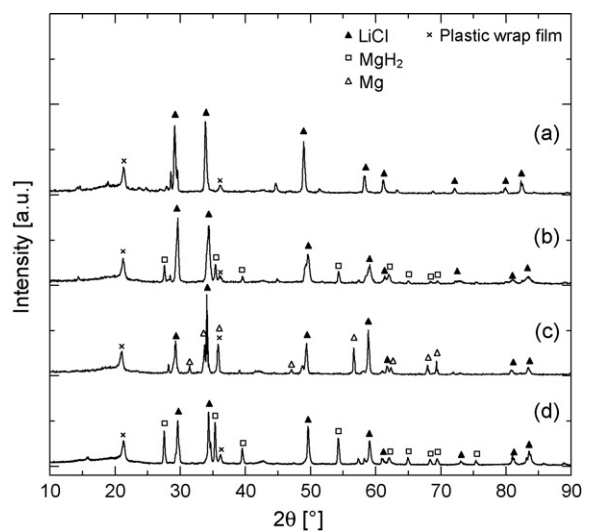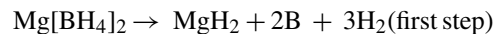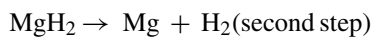
$$Mg[BH_4]_2 \rightarrow MgH_2 + 2B + 3H_2 \text{(first step)}$$

Fig. 8. Powder X-ray diffraction profiles of Li[BH$_4$] and MgCl$_2$ mixture: (a) after heat treatment at 593 K for 3 h, (b) after desorption in vacuum to 593 K, (c) after desorption in vacuum to 623 K and (d) after absorption up to 10 MPa of hydrogen at 623 K, respectively.

$MgH_2 \rightarrow Mg + H_2$(second step)

Taking this result into consideration, the first and the second plateau of the desorption pc-isotherm at 623 K correspond to the desorption from $Mg[BH_4]_2$ to MgH_2 and from MgH_2 to Mg, respectively. This assumption is consistent with the desorbed hydrogen amount ratio (3:1) in the first and the second plateau. Similarly, the absorption plateau in Fig. 6(d) corresponds to the reaction from Mg to MgH_2. The plateau pressure of 1.3 MPa in Fig. 6(d) is almost the same as the equilibrium pressure of Mg/MgH_2 system at the same temperature [18].

4. Conclusions

Li[BH$_4$] reacts with $MgCl_2$ by heat treatment at the temperature >523 K at 10 MPa of hydrogen, where the product contains LiCl and $Mg[BH_4]_2$. Desorption isotherm of the product obtained at 623 K shows two flat plateaus, which indicates that the decomposition of the product after heat treatment consists of a two-step reaction. Using X-ray diffraction analysis, the products of the first and the second decomposition reaction are found to be MgH_2 and Mg, respectively. From the Van't Hoff plot obtained by equilibrium pressures of the first decomposition measured at 563–23 K, the dehydrogenation enthalpy of the first decomposition is found to be $\Delta H = -39.3 \, \text{kJ} \, \text{mol}^{-1} \text{H}_2$, which is lower than that of pure Li[BH$_4$] ($\Delta H = -74.9 \, \text{kJ} \, \text{mol}^{-1} \text{H}_2$). However, only the second reaction step ($MgH_2 \rightarrow Mg$) is reversible at the condition up to 623 K at 10 MPa of hydrogen.

Acknowledgements

References

[1] A. Züttel, Materialstoday Sept. (2003) 24.
[2] B. Bogdanovic, M. Schwickardi, J. Alloys Comp. 253–254 (1997) 1.
[3] A. Züttel, S. Rentsch, P. Fischer, P. Wenger, P. Sudan, Ph. Mauron, Ch. Emmenegger, J. Alloys Comp. 356 (2003) 515.
[4] P. Chen, Z. Xiong, J. Luo, J. Lin, K.L. Tan, Nature 420 (2002) 302.
[5] M. Fichtner, O. Fuhr, O. Kircher, J. Alloys Comp. 356–357 (2003) 418.
[6] J.J. Vajo, S.L. Skeith, F. Mertens, J. Phys. Chem. B 109 (9) (2005) 3719.
[7] M. Aoki, K. Miwa, T. Noritake, G. Kitahara, Y. Nakamori, S. Orimo, S. Towata, Appl. Phys. A 80 (2005) 1409.
[8] K. Miwa, N. Ohba, S. Towata, Y. Nakamori, S. Orimo, J. Alloys Comp. 404–406 (2005) 140.
[9] M. Yoshino, K. Komiya, Y. Takahashi, Y. Shinzato, H. Yukawa, M. Morinaga, J. Alloys Comp. 404–406 (2005) 185.
[10] S. Orimo, Y. Nakamori, G. Kitahara, K. Miwa, N. Ohba, S. Towata, A. Züttel, J. Alloys Comp. 404–406 (2005) 427.
[11] Y. Nakamori, K. Miwa, A. Ninomiya, H. Li, N. Ohba, S. Towata, A. Züttel, S. Orimo, Phys. Rev. B 74 (2006) (045126(1)–045126(9)).
[12] D.S. Stasinevich, G.A. Egorenko, Russian J. Inorg. Chem. 13 (3) (1968) 341.
[13] V.N. Konoplev, V.M. Bakulina, Russian Chem. Bull. 20 (1) (1971) 136.
[14] D. Goerrig, German Patent 1,077,644 (December 27, 1958).
[15] S. Gomes, H. Hagemann, K. Yvon, J. Alloys Comp. 346 (2002) 206.
[16] H.E. Kissinger, Anal. Chem. 29 (1957) 1702.
[17] NEDO international joint research under the "Development for Safe Utilization and Infrastructure of Hydrogen" project progress report; http://www.nedo.go.jp/nenryo/seika/suisoh16-17/seikah_h17_5.pdf.
[18] L.B. Pankratz, Thermodynamic Properties of Carbides, Nitrides, and other Selected Substances, U.S. Dept. of the Interior, Washington, DC, 1995, p. 957.